JOINT INSTITUTE FOR NUCLEAR RESEARCH

Bogoliubov Laboratory of Theoretical Physics

FINAL REPORT ON THE SUMMER STUDENT PROGRAMME

Investigation of a Stack of Josephson Junctions Shunted with LC-Elements

Supervisor:

Dr. Prof. Yuri M. Shukrinov

Student:

Maha Magdy, Egypt
Cairo University

Participation period:

September 14 – October 28

Dubna, 2021

CONTENTS

INTRODUCTION ……3

CHAPTER 1. STACK OF JOSEPHSON JUNCTIONS SHUNTED WITH LC-ELEMENTS ……...5

1.1 Dynamics of a system of coupled Josephson junctions 5

1.1.1 Single Josephson junction ……5

1.1.2 Stack of Josephson junctions ……7

1.2 CCJJ+DC Model ……8

1.3 Effect of shunting LC-elements with a system of coupled Josephson junctions ……10

CHAPTER 2. PHASE DYNAMICS AND CURRENT-VOLTAGE CHARACTERISTIC OF A STACK OF JOSEHSON JUNCTIONS SHUNTED WITH LC-ELEMENTS …….12

2.1 Model and Methods ……12

2.2 Results and Discussions ……13

2.2.1 Double resonance in the system of coupled JJs

2.2.2 Effect of radiation

CONCLUSIONS ……..12

ACKNOLEDGEMENT ……..13

REFERENCES ……14

INTRODUCTION

Strongly anisotropic high-T_c superconductor (HTSC) forms a natural stack of intrinsic Josephson junctions (IJJs) and shows the intrinsic Josephson Effect. Coupling between IJJs in layered high-T_c superconducting materials, such as BSCCO, remains an active topic of investigation. Other than being of theoretical interest as generic models of wave propagation in continuous and discrete media [1], and as models of high-T_c superconductivity [2], IJJs also have several important technological applications. They are currently used, for example, as the basis for the voltage standard [3], and as sources of continuous wave electromagnetic radiation within the elusive terahertz frequency range [4]. Josephson junctions can also model the electrical activity in neurons [5, 6], particularly in memristor-couple-Josephson junction models [7]. And recently, the high frequency nature of the charge oscillation that occur in IJJs has been exploited to develop a device that is theoretically capable of producing artificially created gravitational waves [8].

Intrinsic Josephson effects-tunneling of Cooper pairs between superconducting layers inside of strongly anisotropic layered high-T_c superconductors provide an opportunity to model HTSCs as systems of coupled IJJs and effective way to investigate nonlinear effects and nonequilibrium phenomena in HTSCs. Intrinsic tunnelling is a powerful method for the study of the nature of high-temperature superconductivity, transport along a stack of superconducting layers, and the physics of vortices. It also plays an important role in determining the current-voltage characteristics (CVCs) of tunnelling structures based on HTSCs and the properties of vortex structures in materials.

Parametric resonances of coupled JJs demonstrate a series of effects predicted by numerical simulations [9]. In comparison with the single junction, the system of coupled JJs has a multiple branch structure in its CVCs. The outermost branch of the CVCs has a breakpoint (BP) and a breakpoint region (BPR) before transition to another branch, caused by

parametric resonance [10]. The BP current characterizes the resonance point at which a longitudinal plasma wave (LPW) is created.

In this work we present results of simulations of current-voltage characteristic and phase dynamics of a stack of seven Josephson junctions that is shunted with LC-elements (*L*-inductance, *C*-capacitance). The system was investigated for both periodic and nonperiodic boundary conditions (BC). Effect of electromagnetic radiation was also studied for periodic BC.

CHAPTER 1. STACK OF JOSEPHSON JUNCTIONS SHUNTED WITH LC-ELEMENTS

1.1 Dynamics of a system of coupled Josephson junctions

1.1.1 Single Josephson junction

A Josephson tunnel junction consists of two superconducting electrodes separated by a thin insulating barrier. Brian Josephson predicted that a non-dissipative current can flow in such a device, due to the coherent tunneling of Cooper pairs. In absence of an applied voltage the supercurrent depends solely from the phase difference φ_0 between the two electrodes, according to the first Josephson equation

$$I_s = I_c \sin\varphi. \tag{1}$$

The first Josephson equation defines the current-phase relation of the device, which determines its fundamental properties.

If the phase difference between the two superconducting electrodes changes with time, and so its time derivative is non zero, a voltage difference appears between the superconducting electrodes [11], according to the second Josephson equation

$$V(t) = \frac{\hbar}{2e}\frac{d\varphi}{dt}. \tag{2}$$

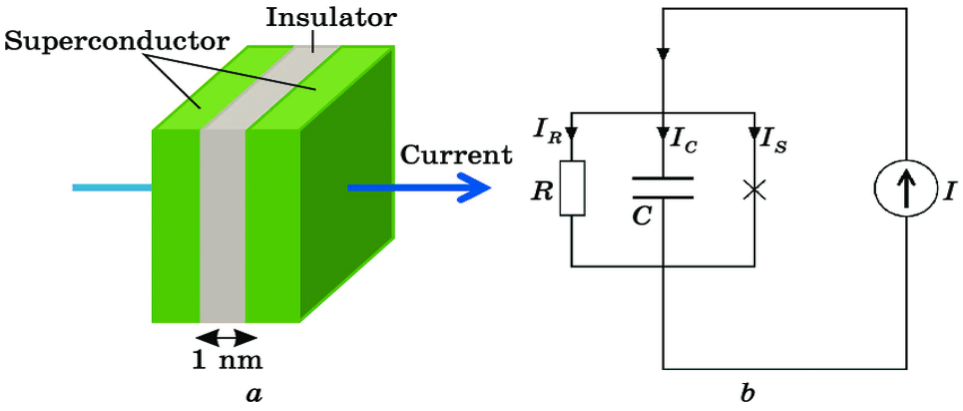

Figure 1. Single Josephson junction: (a) schematic diagram of single SIS Josephson junction, (b) RCSJ equivalent circuit for a real Josephson junction.

A single junction in an electrical circuit can be described by the RCSJ (resistively and capacitively shunted junction). In this model the junction is composed of three branches: one superconducting, one resistive, and one capacitive, connected in parallel. The total current passing through the junction is

$$I = I_c \sin\varphi + \frac{V}{R} + C\frac{dV}{dt}. \quad (3)$$

Writing the above equation in terms of the phase difference and normalize current by I_c and time by the plasma frequency $\omega_p = \sqrt{\frac{2eI_c}{\hbar C}}$, we have

$$i = \sin\varphi + \beta\dot{\varphi} + \ddot{\varphi}, \quad (4)$$

where the dissipation or damping parameter of the junction is given by $\beta = \sqrt{\frac{\hbar}{2eI_c CR^2}}$.

The dc voltage of the junction V is related to mean velocity of the phase by, $\frac{V}{\omega_p} = \left(\frac{\hbar}{2e}\right)\langle\dot{\varphi}\rangle$, also $\frac{V}{I_c R} = \beta\langle\dot{\varphi}\rangle$.

Equation (4) is analog to the equation for the dynamics of the phase of a forced and damped pendulum. Thus, the dynamics of a tunnel junction biased by external current is similar to the behavior of a forced and damped pendulum. This simple analog between the junction and the mechanical pendulum facilitates understanding the main dynamic properties of the system.

The junction is said to be in the superconducting state when V = 0 and $\varphi = \sin^{-1} i_{dc}$. This takes place when the bias current is less than the critical current of the junction $i_{dc} < I_c$. When the bias current exceed the critical current, the phase changes with $V \neq 0$ and the junction is in the resistive state. The current is then oscillating with angular frequency, $\omega_J = \frac{2eV}{\hbar}$. The ratio between frequency and voltage is constant and is given by

$$\frac{V}{\omega_J} = \left(\frac{\hbar}{2e}\right) \tag{5}$$

This is called the a.c. Josephson Effect. The experimental observation of this phenomenon is possible in presence of microwave irradiation of a junction biased with a d.c. current. In this case, the interaction between the microwave signal and the a.c. Josephson current leads to the appearance of current steps at constant voltages. Such steps have been observed for the first time by Shapiro [12] in 1963 and thus are called Shapiro steps. These steps occur at

$$V_n = \frac{nh}{2e}\omega_J, \tag{6}$$

where n is an integer number.

1.1.2 Stack of Josephson junctions

A stack of Josephson junctions consists of N+1 superconducting layers in an anisotropic high-Tc superconductor is shown in Figure 2. Being dynamically coupled, IJJs form natural chains of dissipative oscillators which can sustain several different types of nonlinear waves [13]; including charge travelling waves [14] and longitudinal plasma waves (LPWs) [15]. The LPWs propagate along the c-axis of the crystal and are excited by the periodic action of the Josephson oscillations [16]. For currents above the critical current, when all the junctions are rotating in sync, the angular frequency of rotation ω_J is equal to the average junction voltage. As the dc-bias current is reduced, the average voltage reduces proportionally to the current (obeying Ohm's law), and so also the rotation frequency of the junctions. At a certain frequency, there is a resonance point at which a LPW with half the Josephson frequency is created, i.e. $\omega_J = 2\omega_{LPW}$, where ω_{LPW} is the angular frequency of the LPW. Thus a LPW with a definite wave number is excited in the stack [17]. After the creation of the LPW, and upon further reduction of the bias current, the system enters a so-called break-point region in which it can

exhibit a wide range of interesting dynamic behavior, including quasiperiodic oscillations, and deterministic chaos [18, 19].

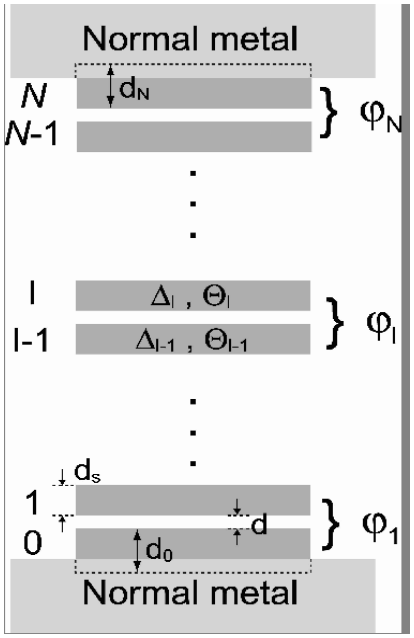

Figure 2. Schematic diagram of a system of intrinsic JJs in HTSCs

1.2 CCJJ+DC Model

A system of N+1 superconducting layers in an anisotropic high-T_c superconductor, which is characterized by the order parameter $\Delta_l = |\Delta|\exp(i\theta_l(t))$ with the time dependent phase $\theta_l(t)$, includes N Josephson junctions [13].

Superconducting layers, which are numbered by l running from 0 to N and characterized by the time-dependent order parameters with moduli Δ_l and phases $\theta_l(t)$, form a system of JJs with phase differences $\theta_l(t) = \theta_l - \theta_{l-1}$; d_s and d are the thicknesses of the superconducting and dielectric layers, respectively.

The thickness of superconducting layers (about 3 A°) in a high-T_c superconductor is comparable with the Debye length r_D of electric charge screening. Therefore, there is no complete screening of the charge in the separate layers, and the electric field induced in each JJ penetrates in the

adjacent junctions. Thus, the electric neutrality of superconducting layers is dynamically broken and, in the case of the alternating current Josephson Effect, a capacitive coupling appears between the adjacent junctions [20]. The absence of complete screening of charge in the superconducting layers leads to the formation of a generalized scalar potential Φ_l of the layer, which is defined of the scalar potential $\emptyset_l$ and the derivative of phase θ_l of the superconducting order parameter as follows: $\Phi_l(t) = \emptyset_l - V_o \frac{d\theta_l}{dt}$, where $V_o = \hbar\omega_p(2e)$, $\omega_p = \sqrt{2I_c/\hbar C_j}$ is the plasma frequency, I_c is the critical current, and C_j is the capacitance of the JJ. The generalized scalar potential is related to the charge density Q_l on the superconducting layer $Q_l = -\frac{1}{4\pi r_D^2}\Phi_l$ [20, 21]. The existence of a relationship between the electric charge Q_l of the *l*th layer and the generalized scalar potential Φ_l of this layer reflects a nonequilibrium nature of the ac Josephson Effect in layered high-T_c superconductors [22].

When an external electric current flows through the stack of coupled Josephson junctions, the superconducting layers are in a nonequilibrium state because of the injection of quasiparticles and Cooper pairs. Since an uncompensated charge exists in the junction, an additional current between superconducting layers should be taken into account. This contribution to the quasiparticle current owing to the difference between generalized scalar potentials is called diffusion current I_{dif}^l. The diffusion current can be represented in the form

$$I_{dif}^l = \frac{\Phi_l - \Phi_{l-1}}{I_c R} = -\frac{(Q_l - Q_{l-1})}{4\pi r_D^2 I_c R} = -\frac{(Q_l - Q_{l-1})}{2e^2 N(0) I_c R} = \beta\dot{\varphi}_l - \beta V_l = -\alpha\beta(V_{l+1} + V_{l-1} - 2V_l) \quad (7)$$

where R is the resistance of the Josephson junction in the resistive state and N(0) denotes the density of states on the Fermi level.

In the absence of the complete screening of the charge in the S layer, the Josephson relation for the gauge invariant phase difference $\varphi_l(t)$ between S layers is generalized to the form

$$\frac{\hbar}{2e}\frac{d\varphi_l}{dt} = V_l - \alpha\left(V_{l+1} + V_{l_{l-1}} - 2V_l\right). \quad (8)$$

Thus, in contrast to the equilibrium case, the derivative of the phase φ_l in the lth junction depends now not only on the voltage $V_l \equiv V_{l,l-1}$ in this junction but also on the voltages in the adjacent ((l-1)th and (l+1)th JJs. The parameter α characterized the capacitive coupling between JJs.

The total current through the system is

$$I_j = C_j \frac{dV_l}{dt} + I_c \sin\varphi_l + \frac{\hbar}{2eR_j}\frac{\partial\varphi_l}{\partial t}, \tag{9}$$

where C_j, V_l, R_j, I_c, and φ_l are the capacitance, voltage, resistance, critical current, and gauge-invariant phase difference of the lth JJ, respectively.

The system of equations (8) and (9) can also be written in the form

$$\partial^2\varphi_l/\partial t^2 = \sum_{l'} A_{ll'}\,(I - \sin\varphi_{l'} - \beta\,\partial\varphi_{l'}/\partial t) \tag{10}$$

where, for nonperiodic boundary conditions (BCs), the matrix A has the form

$$\mathrm{A} = \begin{pmatrix} 1+\alpha G & -\alpha & 0 & \cdots & \\ -\alpha & 1+2\alpha & -\alpha & 0 & \cdots \\ 0 & -\alpha & 1+2\alpha & -\alpha & \\ \vdots & & \vdots & & \\ & & 0 & -\alpha & 1+\alpha G \end{pmatrix} \tag{11}$$

where l' runs over all N junctions, the parameter α gives the coupling between junctions, β is the dissipation parameter ($\beta^2 = \frac{1}{\beta_c}$, where $\beta_c = \omega_p^2 R^2 C^2$ is the McCumber parameter, ω_p is the plasma frequency, and C is the capacity of the junction), I is the external current normalized to the critical current I_c, $G = 1+\gamma$, $\gamma = \frac{d_s}{d_{s0}} = \frac{d_s}{d_{sN}}$, d_s, d_{s0}, d_{sN} are the thicknesses of the middle, first, and last S layers, respectively. In our simulations, we use both periodic and nonperiodic boundary conditions. At nonperiodic BCs it is suggested that the first and the last S layers are in contact with the normal metals, and their effective thicknesses d_{s0} and d_{sN} can be extended to the attached metals. Nonperiodic BCs are characterized by the parameter γ, and the equations for the first and last layers in the

system (10) are different from the equations for the middle S layers. For periodic BCs we consider $V_0 = V_N$ and $V_{N+1} = V_1$ and the matrix A has the form

$$A = \begin{pmatrix} 1+2\alpha & -\alpha & 0 & \dots & -\alpha \\ -\alpha & 1+2\alpha & -\alpha & 0 & \dots \\ 0 & -\alpha & 1+2\alpha & -\alpha & \\ & \vdots & & \vdots & \\ -\alpha & & 0 & -\alpha & 1+2\alpha \end{pmatrix} \quad (12)$$

1.3 Effect of shunting LC-elements on a system of coupled Josephson junctions

One of the main motivations for studying shunted systems of Josephson junctions stems from the fact that, in almost all practical applications or experiments, the junctions have to be connected to some external electrical circuitry, which inevitably introduces stray inductance and/or capacitance in parallel to that of the junctions themselves [22]. Shunting of IJJs by LC-circuit elements also allows for the effective control and manipulation of the resonance features described above. As we have already mentioned, such control could be useful in several superconductive electronic applications [6]. In the shunted systems, when the Josephson frequency ω_J equal to the resonance frequency of the circuit ω_{rc}, the oscillations in Josephson junction are tuned to this frequency. This resonance could manifested itself in the current–voltage characteristic (IV-characteristic) in a variety of ways; such as, steps [23, 24], or humps and dips [25, 26]. LC-shunting leads to a step in the one loop IV-characteristics, when the value of Josephson frequency approaches that of the resonance circuit. As we have discussed previously, the location of this step depends on parameters of the LC-circuit [27]. The existence of steps in the IV-characteristic of various

shunted systems of Josephson junctions has also been reported in a number of experimental and theoretical works [28].

In [27] the possibility of the appearance of an additional parametric resonance, owing to the resonance circuit formed in the system of coupled Josephson junctions with LC shunting, has been demonstrated. As expected, in this case also, a LPW of half the Josephson frequency is excited. The resonance between the Josephson oscillations and those of the LC-circuit triggers the fundamental parametric resonance, which is sustained throughout the region over which there is a transition to inner branches of the IV-characteristic.

A strong LC-shunting effect on the IV-characteristic and voltage–time dependence of Josephson junction under external electromagnetic radiation was also demonstrated in [29]. Crucial changes were found at the resonance condition when the radiation frequency coincided with the Josephson and resonance circuit frequencies, demonstrating a change in the amplitude dependence of the Shapiro step width. Shunting of the junctions provides an extended range of Bessel behavior. For the same microwave source, the Shapiro steps follow the usual Bessel behavior at much smaller radiation power, in comparison to the unshunted case. Such new features of the Shapiro step on the resonance branch are of interest to quantum metrology [30].

CHAPTER 2. PHASE DYNAMICS AND CURRENT-VOLTAGE CHARACTERISTIC OF A STACK OF JOSEHSON JUNCTIONS SHUNTED WITH LC-ELEMENTS

2.1 Model and Methods

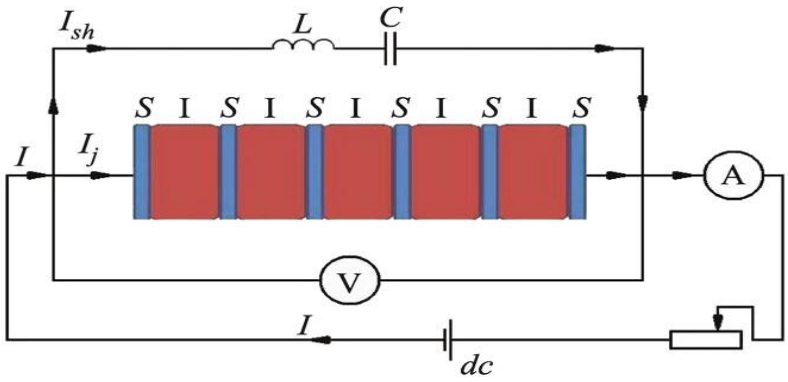

Figure 3. Layout of the system of Josephson junctions with *LC* shunting

Consider the circuit presented in figure 3. In dimensionless form the equations describing this circuit can be written as [27]

$$\begin{cases} \frac{\partial \varphi_l}{\partial t} = V_l - \alpha(V_{l+1} + V_{l-1} - 2V_l), \\ \frac{\partial V_l}{\partial t} = I + I_l^n + A\sin(\omega_R t) - \sin\varphi_l - \beta\frac{\partial \varphi_l}{\partial t} - C\frac{\partial u_c}{\partial t}, \\ \frac{\partial^2 u_c}{\partial t^2} = \frac{1}{LC}(\sum_{l=1}^{N} V_l - u_c\,. \end{cases} \quad (13)$$

Here, all quantities are dimensionless: the bias current I is normalized to the critical current I_c of the JJ, the time is normalized to the inverse plasma frequency ω_p^{-1} (where $\omega_p = \sqrt{2eI_c/C_j\hbar}$; t will be used below for the dimensionless time), the voltages V_l and u_c are normalized to $V_o = \hbar\omega_p/2e$, the shunting capacitance C is normalized to capacitance of JJ C_j, and the shunting inductance L is normalized to $(C_j\omega_p^2)^{-1}$. In the system of equations (13), $\beta = \frac{1}{R_j}\sqrt{\frac{\hbar}{2eI_cC_j}} = \frac{1}{\sqrt{\beta_c}}$ is the dissipation parameter in the JJ, where β_c is the McCumber parameter. We emphasize

that the symbols of dimensionless quantities will be used below for the respective dimensionless quantities.

We note that the shunted system forms a parallel resonance circuit with the resonance frequency

$$\omega_{rc} = \sqrt{\frac{1+NC}{LC}}, \tag{14}$$

where N is the number of JJs in the stack. Furthermore, the electric charge density in the superconducting layers is determined by the difference between the voltages V_l and V_{l+1} across the neighboring insulating layers [9, 31], i.e.

$$Q_l = Q_o \alpha (V_{l+1} - V_l), \tag{15}$$

where $Q_o = \varepsilon_r \varepsilon_o V_o / r_D^2$, ε_r is the relative permittivity and ε_o is the permittivity of free space.

The system of equations (13) was numerically solved by the fourth-order Runge-Kutta method. Its solution at a fixed external current I gives the phase the phase difference $\varphi_l(t)$ and voltage $V_l(t)$ as functions of the time in a certain interval. The method for the calculation of the current-voltage characteristics and time dependence of the electric charge corresponds to the standard scheme and was reported in [31].

2.2 Results and Discussions

2.2.1 Double resonance in the system of coupled JJs

The main feature in the CVC of the shunted JJs is the rc-branch. To clarify the results that follow, we show the rc-branch for a shunted stack of Josephson junctions, corresponding to Eq. (13) with $N = 7$, $L = 30$, $C = 0.005$, $\alpha = 1.5$, $\beta = 0.5$, and nonperiodic BC $\gamma = 0$. The result is presented in figure 4(a). As can be seen, the CVC contains an rc-branch

due to the resonance between the Josephson oscillations and the natural frequency of the resonance circuit, i.e. when $\omega_J \approx \omega_{rc}$. In the case presented in figure 4(a), the rc-branch is the line joining D to E. The position of the rc-branch endpoint (E) corresponds to the voltage V = ω_{rc}= 2.626. This is also the value that can be calculated from Eq.(14), with N = 7, L = 30, and C = 0.005. As it is shown in figure 4(a), the rc-branch appeared at higher value of current compared to what appeared in previous works for systems of periodic BC.

The dependence of the superconducting current I_s on the dc-bias current I is shown in figure 4(b), for the same current sweep path as in figure 4(a). In the zero voltage state I_s first increases linearly along AB, from 0 to 1, and then sharply decreases along BC. Along BC the superconducting current decreases but it does not reach zero at C but It gradually continues decreasing until it reaches zero at D. The current is then increased from point D to point E, which represents the rc-branch. As the bias current is raised further, beyond E, the superconducting current decreases towards zero at F and remained zero along FG with increasing current. Finally, as the bias current is reduced, I_s remained zero until it reaches a maximum at H, where its value peaks at $I_s = 1.43$.

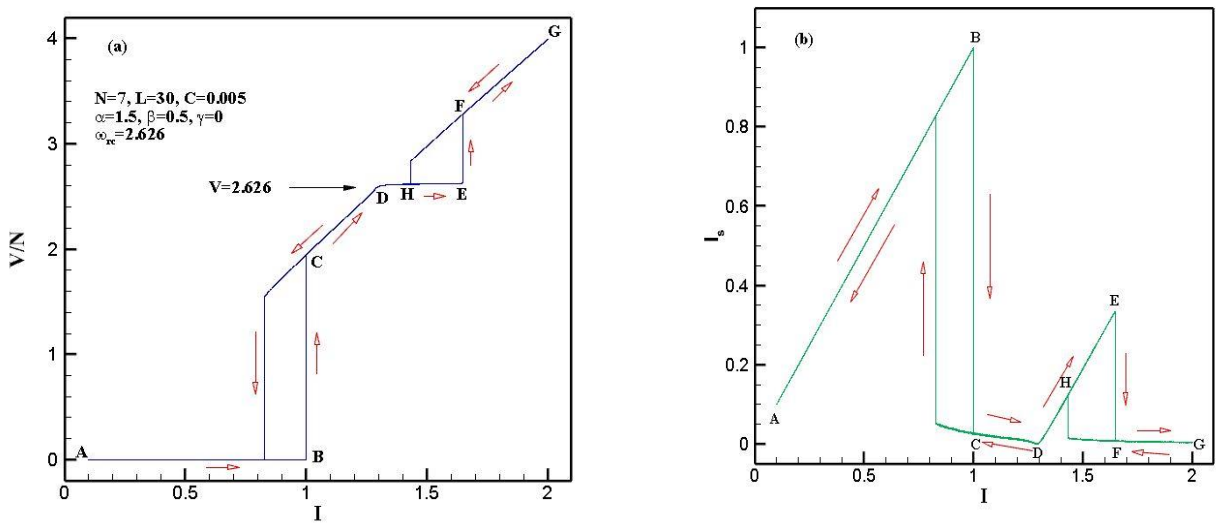

Figure 4. (a) Demonstration of the rc-branch (DE) in the CVC of a shunted stack of seven Josephson junctions, with L=30, C=0.005, and nonperiodic BC $\gamma = 0$. (b) The I-dependence of the average superconducting current $I_s = \langle sin\varphi \rangle_t$.

Figure 5(a) and 5(b) show the temporal dependence of charge on shunted capacitane and the I-dependence of the average current flowing through the shunted capacitance,respectively. The charge in the shunt capacitor is given by th relation

$$Q_c = \frac{u_c}{C} = \frac{1}{C}\left(\sum_{l=1}^{N} V_l - LC\frac{\partial^2 u_c}{\partial t^2}\right). \tag{16}$$

The decrease of the shunt capacitor oscillation amplitude is related to the decrease of the difference in the bracket of equation (16). When the I_{sh} is zero, this means the second term in the bracket of equation (16) to be zero which leads to the Q_c to be maximum. As the I_{sh} increases with increasing bias current, the Q_c begin to decrease.

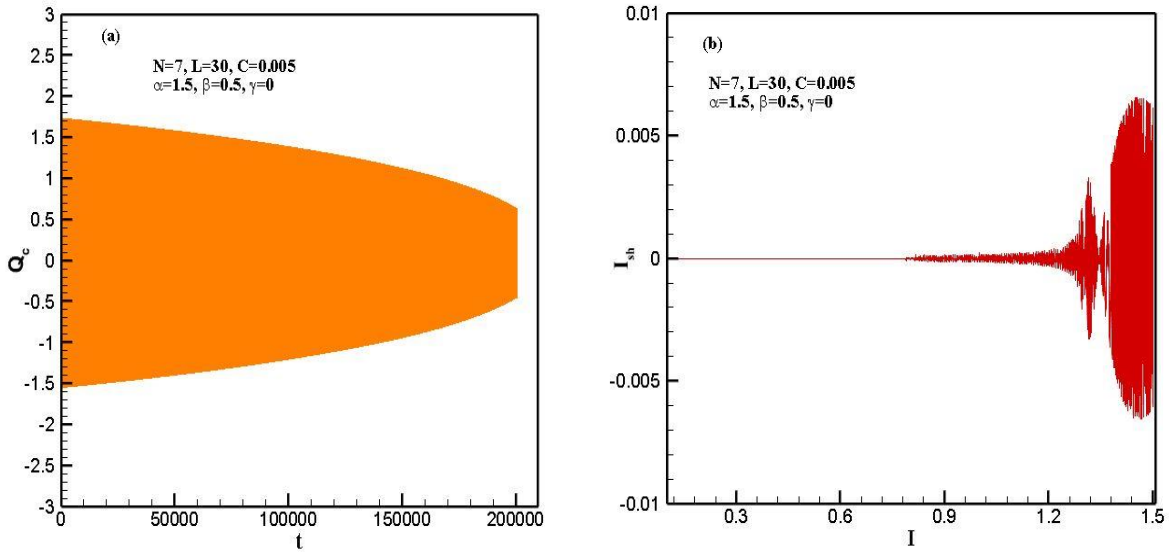

Figure 5. (a) Temporal dependence of charge on shunted capacitance. (b) The I-dependence of the average current flowing through the shunted capacitance $I_{sh} = C\frac{\partial u_c}{\partial t}$.

The time dependence of the maximal charge in the S-layers (green) and the charge on the shunt capacitor (orange), in stacks with different numbers of IJJs, all with C = 0.005, L = 30 and $\gamma = 0.5$ is demonstrated in figure 6(a). From equation (15) it is clear that a growth in charge in the S-layers is accompanied by an increasing phase shift between V_l and V_{l+1}. Figure 6(b) shows an enlarged part of figure 6(a). It is observed that both charges are sinusoidal and have the same wavelength but are out of phase.

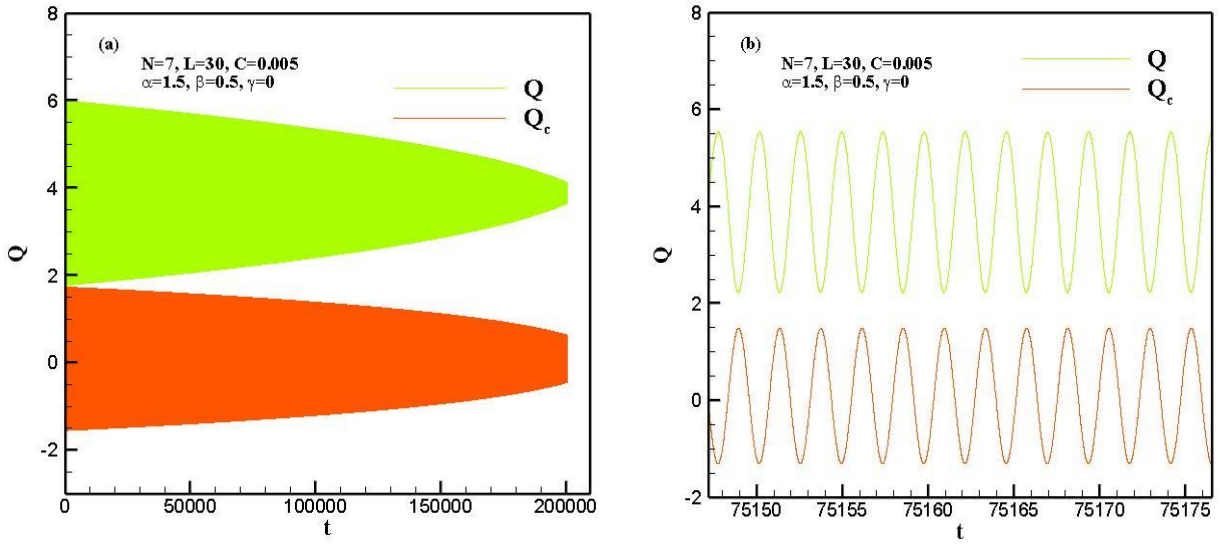

Figure 6. (a) Time series of the maximal charge in the S-layers (green) and the charge on the shunt capacitor (orange), in stacks with different numbers of IJJs, all with C = 0.005 and L = 30. (b) A close-up of the time series of the maximal charge in the S-layers and the charge on the shunt capacitor for those shown in (a).

2.2.2 Effect of radiation

In this section we consider our system under external electromagnetic radiation. Figure 7 shows the IV-characteristic and charge–time dependence for the first S-layer of seven JJs at frequency of radiation $\omega_R = 2.814$, close to the frequency of the resonance circuit, and amplitude A=0.2.

The IV-characteristic (figure 7(a)) has the Shapiro step at the end of the rc-branch (at V=2.83 and its harmonic at V=5.66), so the charging interval does not touch it. Charging of superconducting layers (shown in figure 7(b)) appears in the current interval corresponding to the central part of rc-branch which is lower than a position of the Shapiro step on voltage scale. Below we will discuss the features in the case when charging happens in the current interval, overlapped with a Shapiro step. In the present case, as we have seen in this figure, we have observed different charge oscillations in the superconducting layers for some time regions.

Figures 7(c) enlarge the dependence at the region enclosed with a dashed rectangular, demonstrating the different character of the charge oscillations.

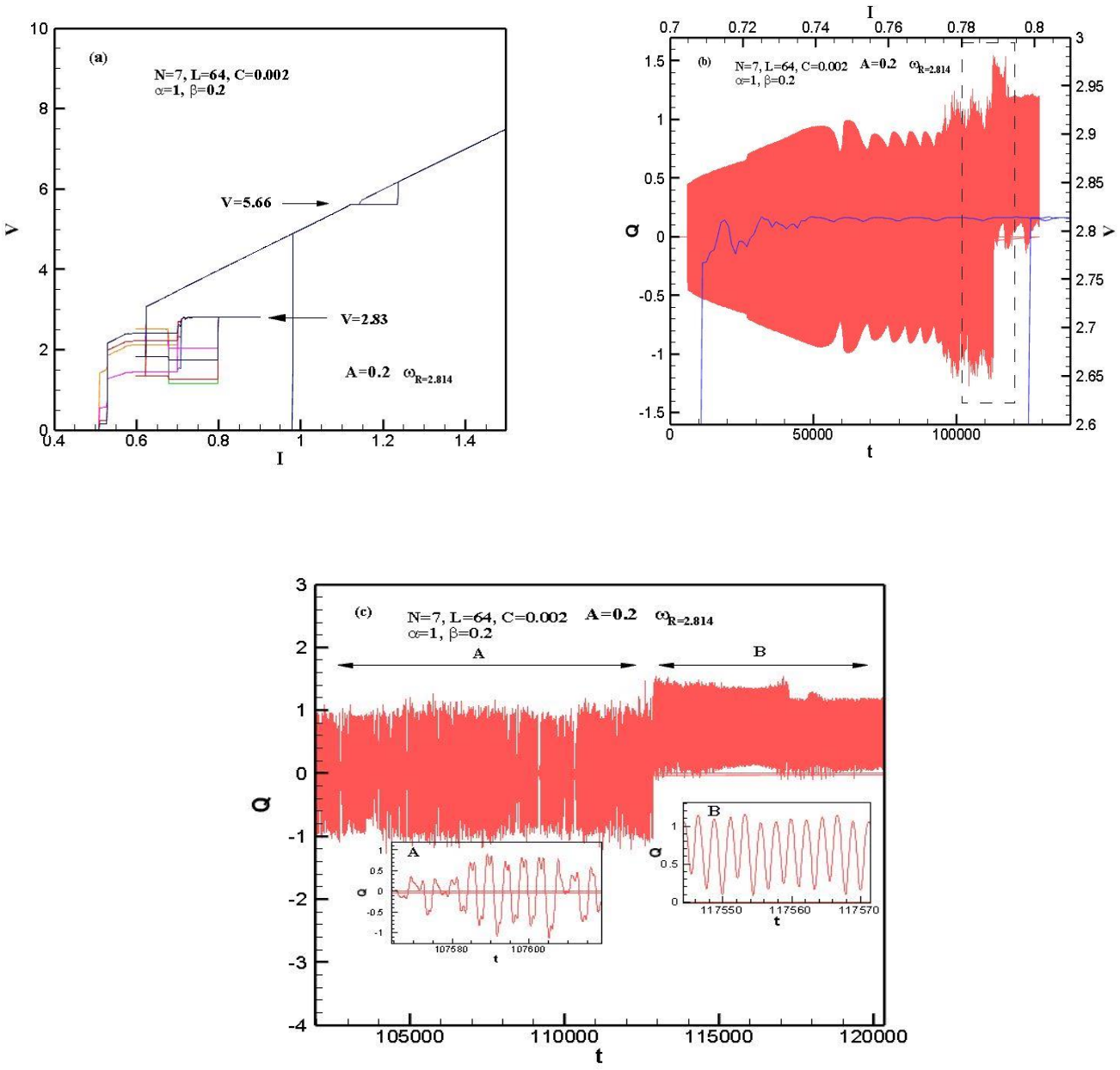

Figure 7. (a) IV-characteristics of seven JJs at $\beta = 0.2, \alpha = 1, L = 64, and\ C = 0.002$ under electromagnetic radiation with frequency $\omega_R = 2.814\ and$ amplitude $A = 0.2$. (b) Charge-time dependence for the first superconducting layer in the stack of the same parameters as in (a). (c) Enlarged parts of charge-time dependence. Insets demonstrate character of charge oscillations in the corresponding regions.

CONCLUSIONS

We have studied the resonance phenomena in Josephson junctions shunted by LC-circuit elements. Our model includes coupling which is appropriate for IJJs that occur in certain high-Tc superconductors. The phase dynamics and IV-characteristics were investigated in as the Josephson frequency approaches the circuit resonance circuit frequency. A realization of parametric resonance and excitation of LPW in the current interval corresponding to the resonance circuit branch was demonstrated. The influence of the external electromagnetic radiation on the IV-characteristics and charge–time dependence demonstrates an effect of different character in the charge oscillations that occur within the S-layers.

ACKNOWLEDGEMENT

I would like to thank Joint Institute for Nuclear Research for giving me the opportunity to participate in the student program and be a part of the scientific group, as well as the Bogoliubov Laboratory of Theoretical Physics. Thanks to my supervisor Shukrinov Yu. M. whose guidance and fruitful discussions assisted me finishing this work. My gratitude for his warm welcome and support for 6 weeks.

REFERENCES

[1] Alfaro-Bittner K., Clerc M.G., Rojas R.G., García-Nustes M.A., Nonlinear Dyn. 98 (2019) 1391.
[2] Kleiner R., H. Wang, Springer Series in Materials Science, vol.286, Springer, Cham, Switzerland, 2019, pp.367–454.
[3] Rüfenacht A., Flowers-Jacobs N.E., S.P. Benz, Metrologia 55 (2018) S152.
[4] Welp U., Kadowaki K., Kleiner R., Nat. Photonics 7 (2013) 702.
[5] Li F., Liu Q., Guo H., Zhao Y., Tang J., Ma J., Nonlinear Dyn. 69 (2012) 2169.

[6] Ma J., Tang J., Nonlinear Dyn. 89 (2017) 1569.
[7] Ma J., Zhou P., Ahmad B., Ren G., Wang C., PLoS ONE 13 (2018) e0191120.
[8] Atanasov V., Phys. Lett. A 384 (2020) 126042.
[9] Shukrinov Y.M., Gaafar M.A., Phys. Rev. B 84 (2011) 094514.
[10] Shukrinov Y.M., Mahfouzi F., Phys. Rev. Lett. 98 (2007) 157001.
[11] Barone, A. Physics and Applications of the Josephson effect / A. Barone, G.Paterno. – John Wiley & sons, 1982.
[12] Shapiro, S. Phys. Rev. Lett. – 1963. – Vol. 11. – P. 80 – 82.
[13] Kleiner R., Steimmeyer F., Kunkel G., Muller P., Phys. Rev. Lett. 68 (1992) 2394.
[14] Kautz R.L., J. Appl. Phys. 52 (1981) 6241.
[15] Kautz R.L., Monaco R., J. Appl. Phys. 57 (1985) 875.
[16] Kautz R.L., J. Appl. Phys. 58 (1985) 424.
[17] Pedersen N.F., Davidson A., Appl. Phys. Lett. 39 (1981) 830.
[18] Irie A., Y. Kurosu, Oya G., IEEE Trans. Appl. Supercond. 13 (2003) 908.
[19] Scherbel J., et al., Phys. Rev. B 70 (2004) 104507.
[20] Koyama T. and Tachiki M. 1996 Phys. Rev. B 54 16183.
[21] Ryndyk D. A. 1998 Phys. Rev. Lett. 80 3376.
[22] Cawthorne A.B., Whan C.B., Lobb C.J., IEEE Trans. Appl. Supercond. 7(2) (1997)2355.
[23] Jensen H. D., Larsen A. and Mygind J. 1990 Physica B 165 1661.
[24] Larsen A., Jensen H. D. and Mygind J. 1991 Phys. Rev. B 43 10179.
[25] Tachiki M., Ivanovic K., Kadowaki K. and Koyama T. 2011 Phys. Rev. B 83 014508.
[26] Zhou T., Mao J., Cui H., Zhao X., Fang L. and Yan S. 2009 Physica C 469 785.
[27] Shukrinov Y. M., Rahmonov I. R. and Kulikov K. V. 2012 JETP Lett. 96 657.
[28] Almaas E. and Stroud D. 2002 Phys. Rev. B 65 134502.
[29] Shukrinov Y. M., Rahmonov I. R., Kulikov K. V. and Seidel P. 2015 Europhys. Lett.110 47001.
[30] Jeanneret B. and Benz S. P. 2009 Eur. Phys. J. Spec. Top. 172 181.
[31] Shukrinov Y. M., Mahfouzi F. and Suzuki M. 2008 Phys. Rev. B 78 134521.